Check for updates

Synthetic Gene Circuits Enable Systems-Level Biosensor Trigger Discovery at the Host-Microbe Interface

Alexander D. Naydich,[a,b] Shannon N. Nangle,[a,b] Johannes J. Bues,[a]* Disha Trivedi,[a] Nabeel Nissar,[a]* Mara C. Inniss,[a]* Matthew J. Niederhuber,[a]* Jeffrey C. Way,[b] Pamela A. Silver,[a,b] David T. Riglar[a,b]*

[a]Department of Systems Biology, Harvard Medical School, Boston, Massachusetts, USA
[b]Wyss Institute for Biologically Inspired Engineering, Boston, Massachusetts, USA

ABSTRACT Engineering synthetic circuits into intestinal bacteria to sense, record, and respond to *in vivo* signals is a promising new approach for the diagnosis, treatment, and prevention of disease. However, because the design of disease-responsive circuits is limited by a relatively small pool of known biosensors, there is a need for expanding the capacity of engineered bacteria to sense and respond to the host environment. Here, we apply a robust genetic memory circuit in *Escherichia coli* to identify new bacterial biosensor triggers responding in the healthy and diseased mammalian gut, which may be used to construct diagnostic or therapeutic circuits. We developed a pipeline for rapid systems-level library construction and screening, using next-generation sequencing and computational analysis, which demonstrates remarkably reliable identification of responsive biosensor triggers from pooled libraries. By testing libraries of potential triggers—each consisting of a promoter and ribosome binding site (RBS)—and using RBS variation to augment the range of trigger sensitivity, we identify and validate triggers that selectively activate our synthetic memory circuit during transit through the gut. We further identify biosensor triggers with increased response in the inflamed gut through comparative screening of one of our libraries in healthy mice and those with intestinal inflammation. Our results demonstrate the power of systems-level screening for the identification of novel biosensor triggers in the gut and provide a platform for disease-specific screening that is capable of contributing to both the understanding and clinical management of intestinal illness.

IMPORTANCE The gut is a largely obscure and inaccessible environment. The use of live, engineered probiotics to detect and respond to disease signals *in vivo* represents a new frontier in the management of gut diseases. Engineered probiotics have also shown promise as a novel mechanism for drug delivery. However, the design and construction of effective strains that respond to the *in vivo* environment is hindered by our limited understanding of bacterial behavior in the gut. Our work expands the pool of environmentally responsive synthetic circuits for the healthy and diseased gut, providing insight into host-microbe interactions and enabling future development of increasingly complex biosensors. This method also provides a framework for rapid prototyping of engineered systems and for application across bacterial strains and disease models, representing a practical step toward the construction of clinically useful synthetic tools.

KEYWORDS synthetic biology, biosensors

Recent advances in our understanding of both the human microbiota and biological engineering techniques have created myriad possibilities for the development of synthetic microbes for *in vivo* clinical applications (1, 2). Because of their proximity to the host and their ability to influence many aspects of human health, intestinal bacteria

are a promising chassis for the deployment of synthetic biological circuits. Such circuits can enable the construction of diagnostic strains that record biological and environmental factors in the intestine, which can be analyzed after transit through the gut to provide a noninvasive survey of an obscure environment. Also compelling is the potential for *in vivo* production of biological therapies. A range of studies have engineered bacteria to serve as potential treatments for inflammation, metabolic diseases, cancer, and infection by producing therapeutic proteins *in vivo* or stimulating immune responses (1, 2).

The majority of studies developing engineered gut bacteria have focused on the expression of therapeutic proteins, either constitutively or by induction with exogenously supplied compounds. However, specific environment- and disease-responsive functions—which could minimize both the metabolic burden of engineered systems on the bacteria and off-target effects on the patient—offer exciting prospects for clinical applications. To this end, recent *in vivo* approaches have developed sensors responding to inflammation (3, 4), intestinal bleeding (5), and pathogen quorum-sensing systems (6, 7). However, the construction of disease-responsive circuits in bacteria has been hindered by the limited number of characterized bacterial systems that can be reliably used as sensors.

Mining the genomes of native gut bacteria is a promising approach for discovering new sensors that respond under conditions of interest, such as in the healthy or diseased gut. To date, these efforts have largely relied on transcriptome sequencing and proteomics of fecal samples. However, to obtain an instantaneous snapshot of bacterial behavior inside the gut using these techniques, invasive sampling is required (i.e., colonoscopy and biopsy). Furthermore, transient or low-abundance signals may not be detected, and any responsive genetic elements identified with these techniques may not function predictably when used in synthetic circuits. Approaches such as *in vivo* expression technology (IVET) and recombinase-based IVET (RIVET) have been used to track *in vivo*-expressed genes noninvasively, primarily focusing on pathogenicity mechanisms in infectious strains (8–11). However, these approaches detect only constitutive expression (for IVET) and may have high false-positive rates. Nevertheless, these technologies show the potential for systems-level approaches to interrogate the behavior of the microbiota.

We have previously developed an approach for noninvasive measurement of bacterial responses in the gut, based on a robust synthetic memory circuit, which records environmental stimuli via a transcriptional trigger (3, 12). When activated, the trigger turns on a memory switch, which can retain the memory-on state for over a week in the gut (12). After the bacteria pass through the host, their memory state can be determined via reporter gene expression, enabling noninvasive readout of transient signals within the gut. The circuit can maintain functional and genetic stability during 6 months' colonization of the mouse gut, demonstrating its suitability for longitudinal studies and its potential to support the development of stable, engineered biosensor strains for *in vivo* deployment (3).

Here, we adapt this memory circuit for parallel, high-throughput screening of hundreds of potential triggers. We apply this method to identify new biosensor triggers responding specifically to the *in vivo* gut environment. Through comparison between healthy mice and those suffering from inflammation, we also identify triggers that respond differentially during disease. Together, these results provide a platform for *in vivo* noninvasive biosensor trigger discovery and longitudinal testing.

(This article was submitted to an online preprint archive [13].)

RESULTS

Bacterial memory as a biosensor trigger screening tool. To enable screening of new potential biosensor triggers in parallel, we modified our previously developed *Escherichia coli* memory circuit, which is based on the λ phage lysis-lysogeny switch (see Fig. S1A in the supplemental material) (12). This modified circuit is referred to as the high-throughput memory system (HTMS) (Fig. 1a). Both the original memory circuit
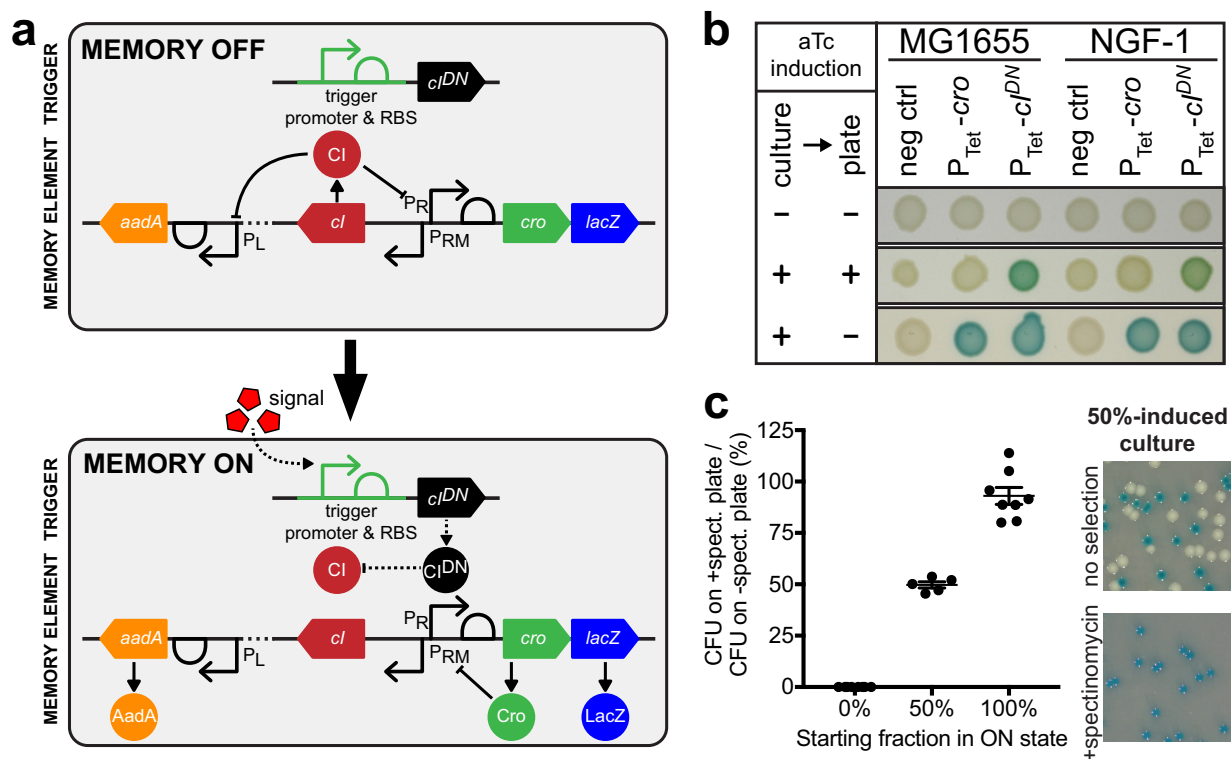
FIG 1 Design of a high-throughput memory system (HTMS). (a) HTMS circuit design in memory-off and memory-on states. (b) Comparison of memory switch induction with *cro* and *cI^DN* triggers illustrates differences in induction dynamics. Control and memory strains with P$_{tet}$ triggers (PAS132, PAS133, PAS807, and PAS808) were grown in liquid media and then spotted on indicator plates, each with or without aTc induction (100 ng/ml). (c) Selection of memory-on HTMS with spectinomycin. Memory-off, memory-on, and 50-50 mixed cultures of PAS810 were plated on indicator plates with or without spectinomycin (inset photo). Graph shows comparison of CFU counts between +spectinomycin and −spectinomycin plates. Error bars represent the SE of eight biological replicates (for 0 and 100%) and five biological replicates (for 50%).

and the HTMS consist of a trigger—based on a transcriptional promoter activated in the presence of a certain stimulus—and a bistable memory switch. The memory-on and memory-off states of the switch correspond to the mutually repressive proteins Cro and CI, which are under the control of the P$_R$ and P$_{RM}$ promoters, respectively. In addition, a β-galactosidase (LacZ) reporter is produced in the memory-on state.

One key modification in the HTMS is the triggering of memory using a dominant-negative mutant of the *cI* gene (*cI^DN*), instead of the *cro* gene used in the original circuit's trigger. In the original circuit, the continued presence of a stimulus can lead to the production of high levels of Cro from the trigger, which can repress both the P$_R$ and P$_{RM}$ promoters and prevent switching to the memory-on state while the stimulus is present. In contrast, the trigger used in the HTMS produces CI^{DN} monomers upon induction, which have an N55K mutation in their DNA-binding region (14). These CI^{DN} monomers dimerize with wild-type (WT) CI monomers expressed in the memory-off state to create heterodimers that are deficient in DNA binding. This leads to derepression of P$_R$ and transition to the memory-on state, even during continued induction of the trigger. As with the CI used in the memory switch, CI^{DN} carries a mutation to prevent RecA-mediated cleavage (ind-) (15).

Use of CI^{DN} in the trigger ensures that there is no delay of switching to the memory-on state in the case of high, or constant, activation of the trigger promoter. To test this, a P$_{tet}$ trigger driving *cI^DN* or *cro* was integrated into *E. coli* K-12 MG1655 and NGF-1 strains containing a memory switch. *E. coli* NGF-1 is a strain originally isolated from the murine gut, which has proven to be an efficient and persistent colonizer and a reliable platform for the deployment of engineered circuits (3, 12, 16). When grown in the presence of a high concentration (100 ng/ml) of anhydrotetracycline (aTc) inducer, *cI^DN*-triggered strains showed switching to the memory-on state, while *cro*-

TABLE 1 Key memory strains used in this study

| Strain	*E. coli* strain	Memory	Trigger promoter/RBS	Trigger gene	Source or reference
PAS132	K-12 MG1655	Original	tet	*cro*	12
PAS133	NGF-1	Original	tet	*cro*	12
PAS807	K-12 MG1655	Original	tet	*cI^{DN}*	This study
PAS808	NGF-1	Original	tet	*cI^{DN}*	This study
PAS809	NGF-1	Original	tet	*cI^{DN}*	This study
PAS810	NGF-1	HTMS	tet	*cI^{DN}*	This study
PAS811	NGF-1	HTMS			This study
PAS812	NGF-1	HTMS	fabR	*cI^{DN}*	This study
PAS813	NGF-1	HTMS	ydiL	*cI^{DN}*	This study
PAS814	NGF-1	HTMS	ydjL	*cI^{DN}*	This study
PAS815	NGF-1	HTMS		*cI^{DN}*	This study
PAS816	NGF-1	HTMS	ynfE15	*cI^{DN}*	This study
PAS817	NGF-1	HTMS	yeaRWT	*cI^{DN}*	This study
PAS818	NGF-1	HTMS	ynfEWT	*cI^{DN}*	This study
PAS819	NGF-1	HTMS	ynfE17	*cI^{DN}*	This study

triggered strains switched only after a subsequent period of growth in the absence of aTc (Fig. 1b).

The original memory circuit expresses a *lacZ* reporter gene for screening on indicator plates (12). To analyze pooled libraries containing many strains with varied trigger promoters, the HTMS also expresses a spectinomycin-selectable resistance gene (*aadA*) in the memory-on state.

This antibiotic-selectable memory maintains response characteristics similar to the original memory switch. To test this, a P$_{tet}$ trigger driving *cI^{DN}* was integrated into strains containing *lacZ* (original) or *aadA*+*lacZ* (HTMS) memory switches, creating PAS809 and PAS810, respectively (see Table 1 for strain list). Strains were induced by aTc (0 to 100 ng/ml) and the response quantified by plating cultures on indicator plates containing X-Gal (5-bromo-4-chloro-3-indolyl-β-D-galactopyranoside), which turns blue in the presence of LacZ, indicating a memory-on state (Fig. S1B). Both strains responded similarly to aTc (original memory 50% effective concentration [EC$_{50}$], 4.1 to 4.6 ng/ml, 95% confidence interval [CI]; HTMS EC$_{50}$, 4.0 to 4.3 ng/ml, 95% CI), confirming the circuit's modularity to additional reporters in the memory-on state.

The HTMS allows faithful selection of memory-on colonies with spectinomycin treatment. Plating of fully memory-off, fully memory-on, and 50-50 mixed cultures of PAS810 on indicator plates with and without spectinomycin further demonstrated that all spectinomycin-selected colonies were also LacZ positive (Fig. 1c). Spectinomycin did not yield false-positive results by inducing memory switching (fully memory-off, 0% $\pm$ 0% standard error [SE], $n = 8$), nor excessive false-negative results through inhibition of memory-on bacterial growth (fully memory-on, 93.0% $\pm$ 4.2% SE, $n = 8$; 50-50 mix, 49.7% $\pm$ 1.5% SE, $n = 5$) (Fig. 1c). Together, these results demonstrate the ability of the HTMS to measure biosensor trigger response and allow selection for downstream pooled analyses.

Biosensor trigger library construction. To build biosensor trigger libraries for genomic integration, we adapted a Tn*7* transposon genome insertion plasmid (17) for rapid Golden Gate assembly (18) of bacterial promoters upstream of the *cI^{DN}* trigger and insertion into the genome of memory bacteria (Fig. 2a and S2). The modularity of this cloning strategy allows for adjustment of trigger sensitivity through incorporation of ribosomal binding site (RBS) variants, which vary the translation rate of mRNA transcripts (Fig. 2a). To test this concept, triggers consisting of a P$_{tet}$ promoter combined with nine synthetic RBS sequences—previously demonstrated to vary widely in their translation strength (19) (Fig. 2a)—were constructed and inserted into the genome of HTMS bacteria, and the HTMS response to varying concentrations of aTc (0 to 100 ng/ml) was characterized (Fig. 2b). The RBS variants differed in their extent of memory induction at 0.1 to 10 ng/ml aTc (EC50 ranging from 0.5 to 4.1 ng/ml for responsive strains), illustrating our ability to tune trigger sensitivity.
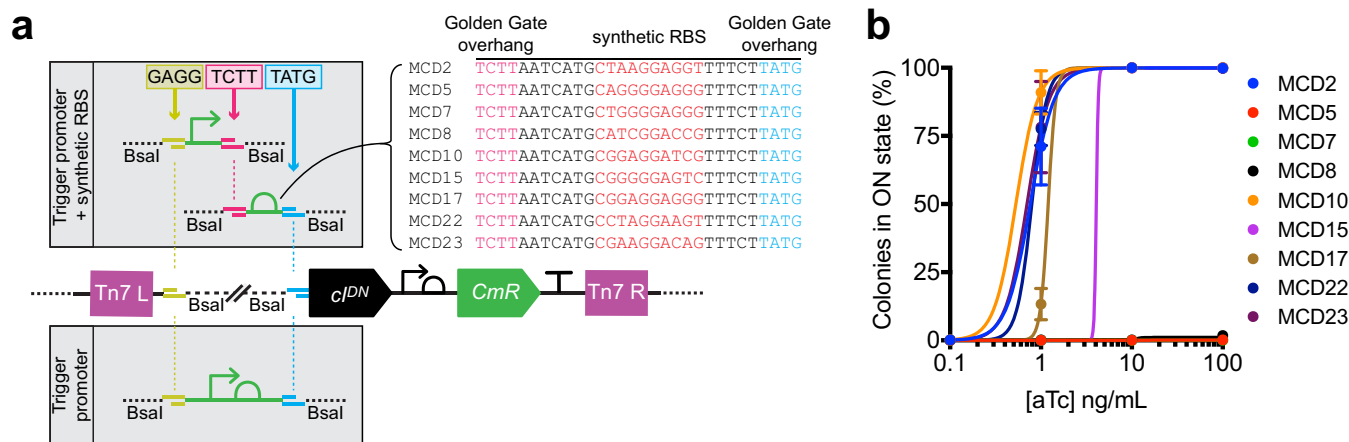
FIG 2 Tuning of trigger sensitivity is achieved through modular incorporation of RBS variants. (a) Strategy for insertion of trigger promoter and RBS variants (19) by Golden Gate assembly (18) into a Tn7 transposon plasmid containing the cl^{DN} gene (Fig. S2). (b) Response curves for RBS variants of a P_{tet}-cl^{DN} trigger in the HTMS chassis strain PAS811 induced with various concentrations of aTc. Memory response was assessed by plating of bacteria on indicator plates after induction with aTc in liquid culture. Error bars represent the SE of three biological replicates.

We explored two approaches for generating biosensor trigger libraries: (i) a comprehensive collection of trigger promoters that would enable screening a wide range of a bacterium's transcriptional responses (MG1655 library) and (ii) a curated collection of promoters with sensitivity variants aimed at detecting inflammation (Nissle 1917 library). Both libraries were assembled into an HTMS-containing *E. coli* NGF-1 strain (PAS811). The comprehensive library was sourced from a previously published collection of 1,600 unique promoters selected from across the genome of *E. coli* K-12 MG1655 (20). Promoters and their wild-type RBSs were amplified by PCR from this collection, assembled into our transposon plasmid, and integrated as triggers into the genome of PAS811, creating a genome-wide library. However, because our method specifically detects off-to-on sensor transitions, the genome-wide library was further subsampled by pooling 500 colonies that were LacZ negative under routine *in vitro* culture to produce a comprehensive, "off-*in vitro*" library. This subsampling maximized sequencing depth for HTMS trigger candidates. Sequencing confirmed the presence of 155 unique strains in this final comprehensive library.

Our second library was constructed with a subset of promoters sourced from the human probiotic *E. coli* Nissle 1917, which are involved in anaerobic respiration of sulfur or nitrogen oxides or nitrate, produced by the gut epithelium during inflammation (21, 22). For each promoter, triggers with the wild-type RBS, as well as with five different synthetic RBSs (MCD5, MCD10, MCD15, MCD17, and MCD23) (19), were included to tune sensitivity. Throughout this study, strains from this library are referred to by an abbreviation consisting of the first gene of the operon from which their trigger is derived and the number of the synthetic RBS used. For instance, "ynfE15" denotes the trigger consisting of the *ynfEFGH* promoter with MCD15. Sequencing confirmed that the assembled library contained 61 unique strains of 66 total designed constructs.

Pipeline for biosensor trigger library screening. To screen for biosensor trigger response, HTMS libraries are exposed to a condition of interest (Fig. 3a), and put through a processing, sequencing and analysis pipeline (Fig. 3b). After exposure, HTMS bacteria are recovered and cultured. The initial culture is split into two and back-diluted, and one of the two new cultures is subjected to spectinomycin selection. After selection, the trigger regions of both cultures are sequenced and analyzed to produce an odds ratio for each trigger promoter in the library, corresponding to that trigger's memory state. To calculate odds ratios, the results are normalized to a positive normalization strain (PAS812) (Fig. 3b). PAS812 is an HTMS strain containing a trigger promoter from the *E. coli fabR* gene, which was observed to be consistently memory-on under *in vitro* culture conditions.
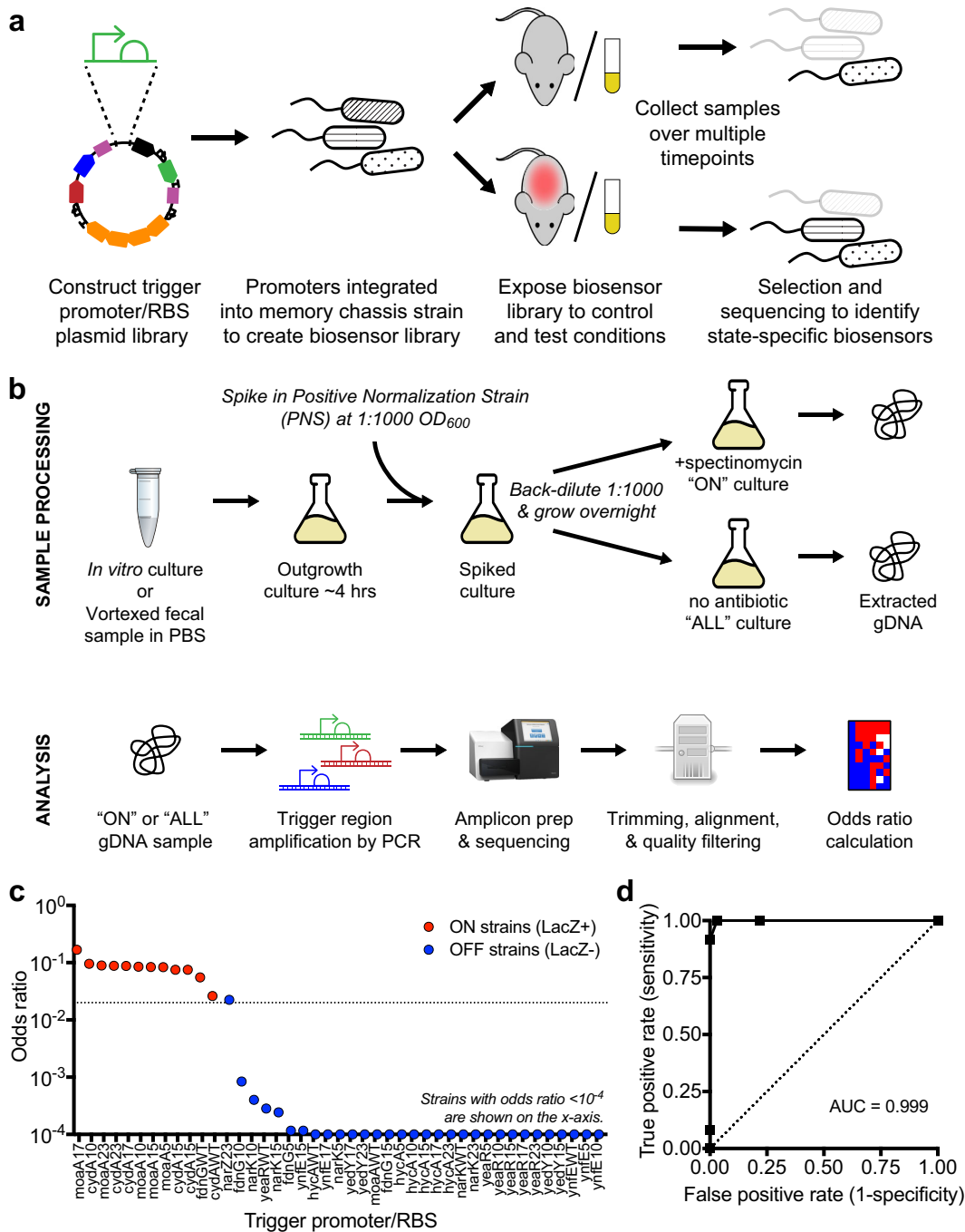
FIG 3 Biosensor trigger library screening and analysis. (a) Libraries were constructed as plasmids, integrated into the genome at single copy, and screened as a pool for differential response to growth in control and test environments. (b) Postexposure library sample processing, selection for memory-on strains, sequencing, and analysis. The consistently memory-on positive normalization strain (PAS812) is spiked in prior to spectinomycin selection and used for the calculation of odds ratios. (c) Calculated odds ratio from *in vitro* pooled growth in LB medium versus memory state assessed by plating individual library strains on LB agar indicator plates. A total of 44 strains subsampled from the Nissle 1917 library were tested. The on-off odds ratio cutoff used in the subsequent *in vivo* screens (0.02) is indicated by the dotted line. (d) Receiver operating characteristic curve for various odds ratio cutoffs as an indicator of memory state.

Library screening faithfully reports biosensor trigger response. To test our library screening pipeline, the Nissle 1917 library was cultured aerobically in liquid media and analyzed to obtain odds ratios as described above. Concurrently, individual strains from this library were grown on indicator plates to assess each strain's *in vitro* memory state directly. Both tests showed strong agreement, with strains that were LacZ

positive also displaying higher odds ratios (Fig. 3c). Receiver operating characteristic analysis confirmed efficient distinction between memory-on and memory-off states, with an odds ratio of approximately 0.02 delimiting the boundary (Fig. 3d). This confirmed our sequencing method as a reliable indicator of biosensor memory state.

Differential biosensor trigger response in the healthy mouse gut. To screen for biosensor trigger response to growth within the murine gut, the MG1655 library was administered to specific-pathogen-free (SPF) mice by oral gavage ($\sim$10^7 bacteria/mouse), and fecal samples were collected over 1 ($n = 2$) or 7 ($n = 3$) days. High library diversity was maintained in both experiments (92 and 82% of strains identified in gavage samples present at the experiment endpoint, respectively; Data Sets S1 and S2). Analysis of HTMS strains recovered from gavage suspension and fecal samples identified 23 unique strains that responded specifically to growth within the gut (gavage: odds ratio < 0.02; fecal samples: ≥1 time point with an odds ratio ≥ 0.02, and $P < 0.05$) (Fig. 4a and b; Data Sets S1 and S2). Five strains (containing *ydiL*, *ydjL*, *gatY*, *gcvA*, and *ubiG* triggers) were detected in the memory-on state in at least four of five mice. The two most consistent responders (*ydjL* and *ydiL* triggers) were selected for follow-up testing.

To validate the response of the *ydiL* and *ydjL* triggers during gut transit, memory bacteria containing these triggers (*ydiL*, PAS813; *ydjL*, PAS814) or a promoterless *cI*^{DN} gene (negative control, PAS815) were administered to SPF mice as monocultures. Fecal samples were collected and analyzed over the subsequent 5 days. Culture on indicator plates demonstrated an absence of memory activation in all three strains prior to gavage. However, when recovered from fecal samples, PAS813 and PAS814 colonies were consistently memory-on, confirming activation during gut transit (at day 2, PAS813: 51% ± 8% SE; PAS814: 30% ± 4% SE; negative control: 0% ± 0% SE; $n = 3$) (Fig. 4c).

The Nissle 1917 library was also screened to discover promoters responding in the healthy mouse gut. Testing of the Nissle 1917 library over 5 days following gavage ($\sim$10^7 bacteria/mouse) identified 11 strains that specifically responded to *in vivo* growth (Data Set S3). Ten of these, derived from three unique promoters (*ynfEFGH*, *torCAD*, and *yeaR-yoaG* operons) registered a memory-on state in the majority of time points and all mice tested ($n = 4$) (Fig. 4d and e). Promoter response was similar during parallel analysis in the inflamed mouse gut ($n = 4$; see below and Fig. 5 for experimental details), further validating these results (Fig. S3 and Data Set S3).

RBS variation to adjust trigger sensitivity affects *in vivo* sensing capacity. Variation in sensor response based on trigger RBS was most notably observed with the *ynfEFGH* promoter: WT, MCD5 and MCD17 RBSs showed no response throughout the screening experiment, whereas MCD10, MCD15, and MCD23 registered as memory-on in 100%, 100 and 94% of time points, respectively (Data Set S3, "–DSS" columns). To validate these findings, ynfE15 (PAS816), yeaRWT (PAS817), and ynfEWT (PAS818, used here as a negative control) strains were administered to SPF mice as monocultures, with memory state determined by culture on indicator plates (at day 2, ynfE15: 99% ± 1% SE; yeaRWT: 31% ± 4% SE; ynfEWT: 0% ± 0% SE; $n = 3$) (Fig. 4f). Of note, changing the *ynfE* trigger RBS from WT to MCD15 increased memory-on rate in the gut from 0% to nearly 100%.

Together, these results demonstrate the ability for HTMS analysis to rapidly identify biosensor triggers *in vivo* and the power of varying trigger sensitivity to tune the strength of biosensor strain response.

***In vitro* induction of *in vivo*-responding biosensor strains.** The Nissle 1917 library includes some promoters with previously characterized induction conditions. We tested induction of *ynfEFGH* promoter trigger memory strains, which derive from an operon known to respond to low nitrate (through repression by phosphorylated NarL) and anaerobic (through FNR activation) conditions (23). When grown anaerobically in rich media, PAS816 (ynfE15) produced a memory response (13.3% ± 0.7% SE, $n = 7$). With added nitrate (20 mM) or under aerobic conditions, PAS816 produced no response
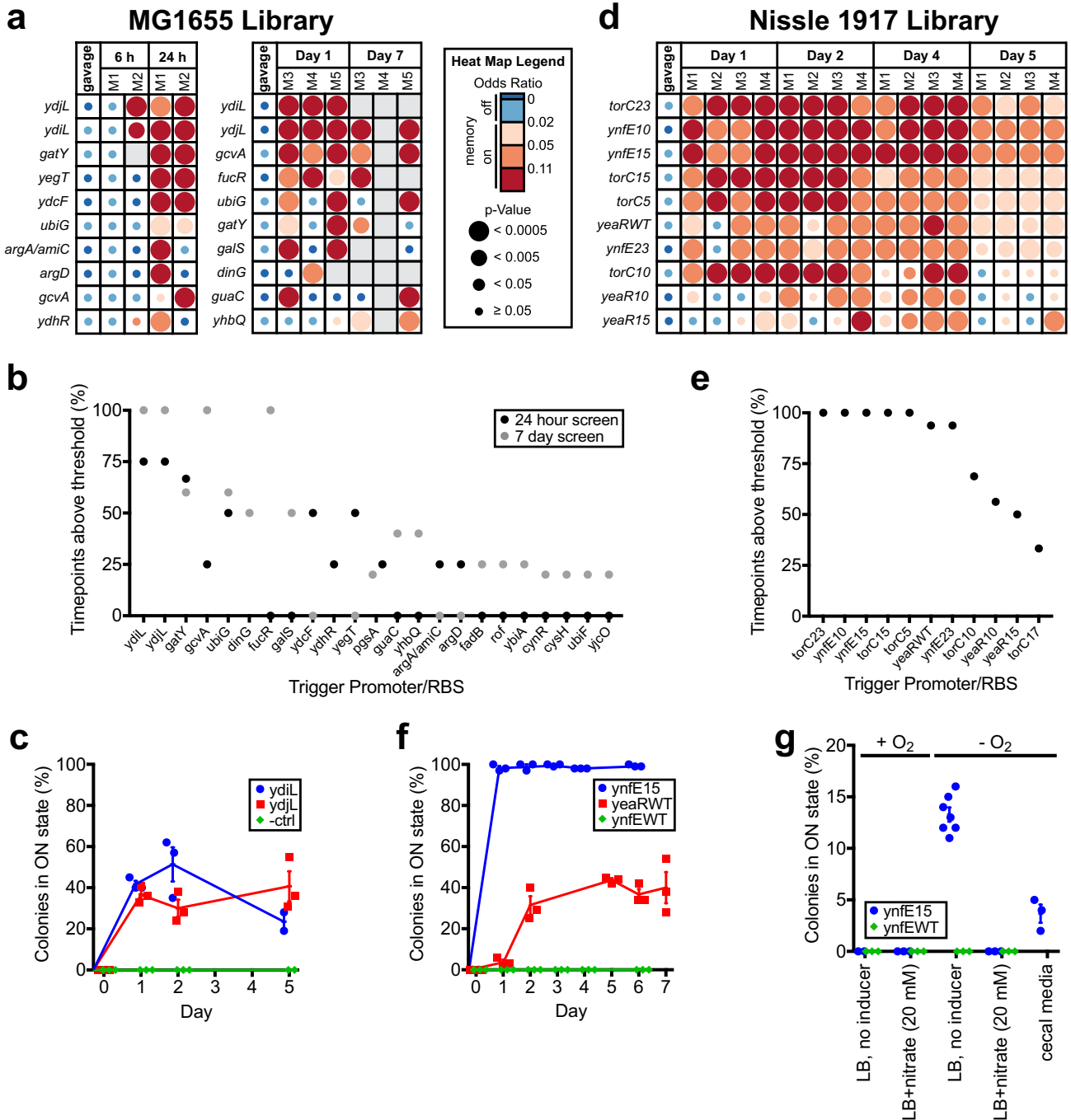
FIG 4 Library screening and individual sensor testing identifies biosensor triggers responding in the *in vivo* gut environment. (a) Screen of MG1655 library in BALB/c mice over 1 day (left, *n* = 2) and over 7 days (right, *n* = 3). Odds ratio heat maps of the top 10 hits are shown, sorted by percentage of positive time points (odds ratio ≥ 0.02 and *P* < 0.05) over the course of the experiment. Blank spaces on heat maps represent insufficient sequencing coverage. See Data Sets S1 and S2 for full results. (b) Percentage of positive time points (odds ratio ≥ 0.02 and *P* < 0.05) for all positive hits from two MG1655 library screens (top 10 shown in panel a). (c) Response of individual strains from MG1655 library in healthy mice. HTMS strains containing triggers ydiL (PAS813), ydjL (PAS814), and an empty trigger (PAS815) were administered as monocultures to BALB/c mice (*n* = 3). Memory response was assessed by plating of HTMS bacteria recovered from fecal samples on indicator plates. Error bars represent the SE. (d) Screen of Nissle 1917 library in C57BL/6J mice (*n* = 4) over 5 days. An odds ratio heat map of the top 10 hits is shown, sorted by the percentage of positive time points (odds ratio ≥ 0.02 and *P* < 0.05) over the course of the experiment. Blank spaces on the heat map represent insufficient sequencing coverage. See Data Set S3 for full results. (e) Percentage of positive time points (odds ratio ≥ 0.02 and *P* < 0.05) for all hits from Nissle 1917 library screen in healthy mice (top 10 shown in panel d). (f) Response of individual strains from Nissle 1917 library in healthy mice. HTMS strains containing the ynfE trigger with MCD15 (PAS816), the yeaR trigger with its WT RBS (PAS817), and the ynfE trigger with its WT RBS (PAS818) were administered as monocultures to C57BL/6J mice (*n* = 3). The memory response was assessed by plating of HTMS bacteria recovered from fecal samples on indicator plates. Error bars represent the SE. (g) Response of the ynfE15 trigger (PAS816) and ynfEWT trigger (PAS818) strains to *in vitro* growth in rich media with or without 20 mM nitrate, with or without oxygen, and in the presence of mouse cecum fluid medium (ynfE15 strain only). Memory response was assessed by plating on indicator plates after growth in liquid culture. Error bars represent the SE. (*n* = 7 for ynfE15 strain in −O$_2$, LB, no inducer condition; *n* = 3 for all other conditions.)
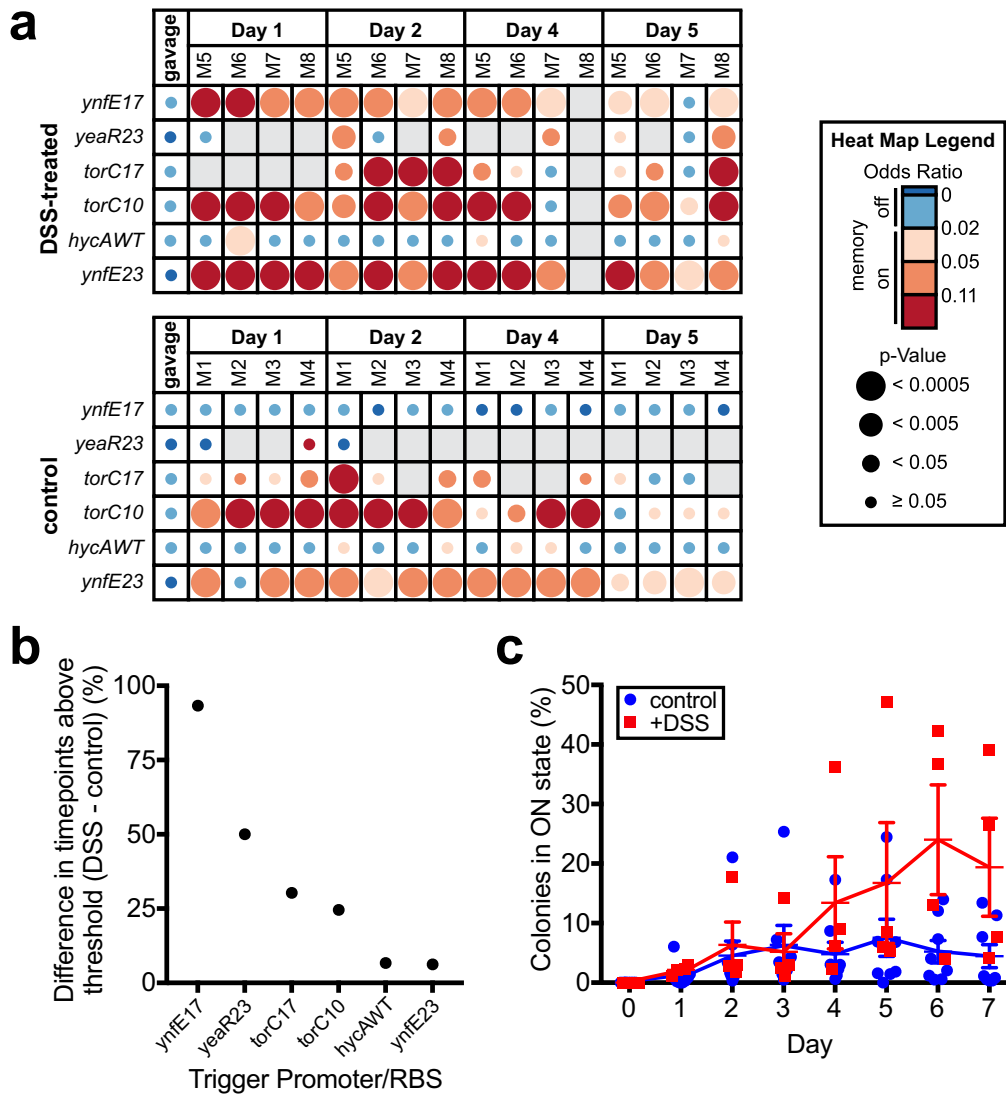
FIG 5 Library screening and individual sensor testing identifies biosensor triggers with increased response during inflammation. (a) Screen of Nissle 1917 library in DSS-treated C57BL/6J mice ($n = 4$) over 5 days and comparison to results of previous screen in healthy C57BL/6J mice ($n = 4$, control group; also see Fig. 4d and e). To identify sensors responding more strongly to the inflamed state, the fraction of time points registering memory-on (odds ratio ≥ 0.02 and $P < 0.05$) in the control group was subtracted from the fraction in the DSS-treated group for each strain in the library, and strains were sorted according to the greatest difference between the two groups. An odds ratio heat map of the six strains registering a positive difference between the two groups is shown. Blank spaces on the heat map represent insufficient sequencing coverage. See Data Set S3 for full results. (b) Differences in percentage of positive time points (odds ratio ≥ 0.02 and $P < 0.05$) between DSS-treated and control group mice for strains showing a positive difference between the two groups (heat map shown in panel a). (c) Response of HTMS strain containing the ynfE trigger with MCD17 (PAS819) in DSS-treated mice ($n = 4$) and healthy mice ($n = 8$). Memory response was assessed by plating of HTMS bacteria recovered from fecal samples on indicator plates. Error bars represent the SE.

($-O_2$/+nitrate: 0% $\pm$ 0% SE; +O_2/+nitrate: 0% $\pm$ 0% SE; +O_2: 0% $\pm$ 0% SE; $n = 3$) (Fig. 4g), consistent with previous literature reports of *ynfEFGH* promoter behavior (23). In addition, no response was observed from PAS818 (ynfEWT) in any of these conditions (all conditions: 0% $\pm$ 0% SE, $n = 3$) (Fig. 4g), suggesting that it is less sensitive than PAS816 (ynfE15), which is consistent with our *in vivo* results. ynfE15 was also shown to respond to *in vitro* growth in cecal contents (3.7% $\pm$ 0.9% SE, $n = 3$) (Fig. 4g).

Identification of disease-specific biosensor triggers. To look for sensors responding differentially to disease, we compared the response of the Nissle 1917 library in healthy mice ($n = 4$; as previously displayed in Fig. 4d and e and Data Set S3) to a

murine intestinal inflammation model (Fig. 5a and b, Fig. S4, and Data Set S3). After library gavage, SPF mice were provided water containing 4% (wt/vol) dextran sulfate sodium (DSS) *ad libitum* for 5 days, and HTMS analysis was performed on fecal samples throughout. Weight loss (Fig. S4A), colon length reduction at endpoint (Fig. S4B), and increased *E. coli* CFU counts (Fig. S4C) were all consistent with increasing inflammation throughout the experiment. Six strains registered memory-on at more time points in the DSS-treated group than in the control group (Fig. 5a and b). In particular, the ynfE17 trigger strain (PAS819) responded specifically in DSS-treated mice (control: no response; DSS-treated: 93% of time points with an odds ratio $\geq$ 0.02 and $P <$ 0.05) (Fig. 5a and b; Data Set S3).

To validate ynfE17 (PAS819) response to inflammation, the strain was administered to SPF mice as a monoculture, after which a subset of the mice was provided water containing 4% DSS. Fecal samples were cultured for memory bacteria on indicator plates for 7 days after gavage. As above, body weights (Fig. S4D), post-dissection colon lengths (Fig. S4E) and CFU counts of HTMS bacteria (Fig. S4F) reflected increased inflammation in DSS-treated mice. Confirming the screen results, ynfE17 showed increased response in DSS-treated mice compared to untreated controls, with the greatest difference between groups at days 6 and 7 (at day 6, +DSS: 24% $\pm$ 9% SE, $n = 4$; control: 5% $\pm$ 2% SE, $n = 8$) (Fig. 5c). The strong response of PAS819 in the absence of DSS in one of the control group mice indicates that *in vivo* conditions other than DSS treatment can activate the ynfE17 trigger. *In vitro* anaerobic growth both in rich media and in cecal contents did not induce ynfE17 (rich media: 0 $\pm$ 0% SE, $n = 7$; cecal contents: 0 $\pm$ 0% SE, $n = 3$), in contrast to ynfE15 (Fig. 4g), suggesting a lower nitrate threshold for ynfE17 activation and that individual bacteria experience low nitrate conditions within the inflamed mouse gut.

DISCUSSION

Here, we have expanded the use of a robust genetic memory circuit to assess the *in vivo* responses of multiple bacterial sensors in parallel. The original memory circuit (12) was altered to allow off-to-on transitions in the presence of constant induction and to enable selection of memory-on strains from pooled libraries using spectinomycin. We developed a screening, sequencing, and analysis pipeline to efficiently identify *in vivo*-responding trigger-RBS combinations. Tests conducted with both comprehensive and curated libraries containing hundreds of sensors demonstrated that our method is an effective, noninvasive way to identify new biosensor triggers responding in the gut. We identified and validated biosensor triggers responding to growth in the healthy mouse gut and preferentially in inflamed conditions. Together, these results demonstrate the power of tuning trigger sensitivity to physiological responses and for the HTMS to assess unique features of the mammalian gut environment *in vivo*.

One advantage of our method is its ability to discover sensors that could not be rationally designed based on existing knowledge, presenting an opportunity to apply the rapidly increasing but largely uncharacterized genetic diversity identified through microbiome sequencing. For instance, the two validated healthy-gut sensors from our *E. coli* MG1655 library (PAS813 and PAS814) are derived from operons with largely uncharacterized function and regulation. PAS814 is triggered by the promoter of the *ydjLKJIHG* operon, which putatively includes a kinase, a transporter protein, two dehydrogenases, an aldolase and an aldo-keto reductase. Only the activity of the aldo-keto reductase, YdjG, has been confirmed through reduction of methylglyoxal (24, 25). Interestingly, a previous analysis of *E. coli* protein expression in germfree mice showed that YdjG was expressed 3.5-fold higher in the cecum than *in vitro* (26). Another gene which has been studied in this operon, *ydjK*, may play a role in osmotolerance, showing a 50% increased growth rate in high-salt media when overexpressed in *E. coli* (27). It is not known whether methylglyoxal or osmotic stress can directly trigger transcription of the *ydjLKJIHG* operon. However, methylglyoxal occurs in many foods and is also produced by intestinal bacteria (28); it can also inhibit bacterial growth, suggesting a possible motivation for expression of *ydjLKJIHG* in the gut.

Promoters derived from three unique Nissle 1917 operons (*ynfEFGH*, *torCAD*, and *yeaR-yoaG*) showed memory response in the healthy mouse gut (Fig. 4d and e). The *ynfEFGH* operon encodes a DMSO reductase which has also been shown to reduce selenate (29, 30). It is activated by FNR under anaerobic conditions and repressed by phosphorylated NarL in the presence of nitrate (23), which was further confirmed by our *in vitro* tests with PAS816 (Fig. 4g).

Tuning of trigger sensitivity (e.g., by RBS modulation) is important for generating responses to physiological conditions of interest and for successful application in synthetic engineered circuits. As we observed, RBS tuning can be used to increase the response of the ynfE promoter to as high as 100% in healthy mice (PAS816; Fig. 4f), and to adjust the response to distinguish the inflamed gut state (PAS819; Fig. 5c). Importantly, the sensors we identify can be used directly in downstream applications with the memory circuit. This provides an engineering advantage over any responsive genetic elements identified through analysis in their native context, for which incorporation into synthetic circuits would routinely require additional optimization.

Inflammation leads to an increase in nitric oxide produced by the host, which generates nitrate in the intestine (31). However, because the ynfE promoter is activated by a decrease in nitrate, our results suggest that DSS-induced inflammation may lead to lower levels of free nitrate available to *E. coli* NGF-1, possibly due to increased local competition for nitrate via respiration by NGF-1 and other *Enterobacteriaceae*. This idea is supported by our observation of increasingly higher NGF-1 bacterial loads in fecal samples of DSS-treated mice (Fig. S4C and F), suggesting a bloom of *E. coli*—and potentially other *Enterobacteriaceae* capable of nitrate respiration—correlated with increasing duration of DSS treatment. This is consistent with previous descriptions of *E. coli* experiencing a growth advantage due to anaerobic respiration of host-derived nitrate (31). Thus, we hypothesize that PAS819 responds in DSS-treated mice specifically through sensing inflammation-induced changes in its own microenvironment.

The HTMS enables both the recording of transient signals and the amplification of low-abundance signals through antibiotic selection. These features serve as a useful complement to other techniques, such as meta-transcriptomic or -proteomic studies which capture an instantaneous snapshot of total RNA or protein content. Screening of broad libraries increases the chances of discovery of new, uncharacterized sensors. Combining comprehensive libraries with RBS tuning would further increase the chances of identifying triggers specific to conditions of interest. Our use of the *E. coli* NGF-1 strain as a chassis allows reliable colonization of the mouse gut without requiring antibiotic maintenance, leading to retention of high bacterial loads and high library complexity in fecal samples even after long periods in the gut.

For clinical applications, an expanded arsenal of characterized sensors presents opportunities to construct more complex disease-responsive circuits. For instance, the combination of multiple redundant sensors would increase response accuracy and specificity under variable *in vivo* conditions, while complementary sensors may allow "fingerprinting" of different disease states. An exciting possibility is the use of more complex logic and signal processing within a single engineered strain, which may sense multiple inputs and produce anti-inflammatory, antimicrobial, or other therapeutic proteins only when a precise set of conditions is satisfied (2). Sensors responding differentially based on localization within the intestine may create opportunities for more targeted drug delivery or for the construction of new safety and containment mechanisms—another important consideration in the deployment of engineered organisms.

The potential to engineer synthetic circuits into commensal gut bacteria is a promising new approach to the management of intestinal disease. Synthetic biology is just beginning to tap into the evolutionary breadth of capabilities found in natural systems, and our method represents a practical means for expanding the toolkit of useful sensors for *in vivo* application.

MATERIALS AND METHODS

Media and culture conditions. Unless otherwise mentioned, bacterial cultures were grown at 37°C in LB broth or agar (10 g/liter NaCl, 5 g/liter yeast extract, 10 g/liter tryptone). Mixed liquid cultures (i.e., libraries) were grown in LBPS, which contains Peptone Special (Sigma) instead of tryptone. To quantify memory response on indicator plates, agar was supplemented with 60 μg/ml X-Gal.

High-throughput memory system construction. The spectinomycin resistance gene, *aadA*, was added downstream of the P_L promoter in the original memory switch (12) by overlap extension PCR and genomically integrated by λ Red recombineering (32) into *E. coli* TB10 (33) between *mhpR* and *lacZ*, driving endogenous *lacZ* as a memory-on reporter. From TB10, transfer into streptomycin-resistant *E. coli* NGF-1 was done by P1*vir* transduction.

Biosensor strain and library construction. All triggers were cloned into pDR07 (Fig. S2), a Tn*7* transposon insertion plasmid derived from pGRG36 (17). BsaI sites directly upstream of *cI^DN* allow modular insertion of promoter–RBS sequences via Golden Gate assembly (18) (Fig. 2a). Assembled trigger plasmids were electroporated into PAS811. After recovery (90 min, 30°C in SOC medium) transformants were selected overnight (30°C in LB-ampicillin [100 μg/ml]). Cultures were then back-diluted 1:100 into LB-chloramphenicol (25 μg/ml) plus 0.1% arabinose to induce transposase genes. After >6 h at 30°C, temperature-sensitive pDR07 plasmids were cured from integrants by 1:100 back-dilution into LB-chloramphenicol and >6 h growth at 42°C. This cure step was repeated a second time. Plasmid loss was confirmed by restreaking on LB-ampicillin agar.

For individual strains, post-cure cultures were plated on LB-chloramphenicol agar and attTn*7* integrations confirmed by PCR and Sanger sequencing. For pooled libraries, library composition was confirmed by Illumina MiSeq sequencing of pooled PCRs of trigger regions.

Assessment of memory state by LacZ assay. Cultures or fecal supernatants containing memory bacteria were plated on agar plates containing streptomycin (200 μg/ml), chloramphenicol (34 μg/ml), and X-Gal (60 μg/ml). The percentages of memory-on colonies were assessed by counting blue (on) and white (off) colonies.

***In vitro* induction.** Overnight liquid cultures were back-diluted 1:100 into fresh media containing inducer, followed by 4 h growth and plating on X-Gal agar. For induction in cecal contents, contents of ceca from three female SPF C57BL/6J mice and suspended at 10% (wt/vol) in phosphate-buffered saline (PBS). Suspensions were vortexed 90 s and centrifuged for 3 min at 4,300 relative centrifugal force (rcf). The supernatant was recovered, supplemented with 200 μg/ml streptomycin and used for growth of HTMS bacteria.

For anaerobic inductions, prereduced anaerobic medium was used, and growth occurred in an anaerobic chamber (Coy Laboratory Products) under 7% H_2, 20% CO_2, and 73% N_2.

***In vivo* induction of strains and libraries.** The Harvard Medical School Animal Care and Use Committee approved all animal protocols. Experiments were conducted in female 7- to 14-week-old BALB/c mice (Charles River; MG1655 library) or C57BL/6J mice (Jackson; Nissle 1917 library). Before experiments, all mice were confirmed to be free of native streptomycin- and chloramphenicol-resistant flora. Food and water were removed ~4 h before each gavage; water was replaced immediately, and food was replaced <2 h after gavage.

One day prior to bacterial gavage, mice were provided streptomycin (20 mg in PBS) by oral gavage. The next day, overnight cultures of memory strains or libraries were washed once and then diluted 10-fold in PBS and administered by gavage (100 μl; ~10^7 bacteria/mouse).

Gavage suspension and fecal samples were plated to track bacterial load and, for individual strains, to assess memory state. Libraries were processed according to the postexposure processing protocol below. To plate fecal bacteria, samples were suspended at 100 mg/ml in PBS, vortexed 5 min, and centrifuged 20 min at 4 rcf to obtain fecal supernatant.

For inflammation experiments, water containing 4% DSS (36,000 to 50,000 molecular weight; MP Biomedicals, catalog no. 160110) was substituted 2 h after bacteria administration. Mice were dissected at the end of the experiment to measure colon length.

Postexposure library processing. Fecal supernatant or *in vitro* culture was diluted 1:100 into LBPS-chloramphenicol (25 μg/ml) to achieve ~10^6 CFU/ml. Concurrently, an overnight culture of the positive normalization strain, PAS812 was back-diluted 1:100 into LBPS-chloramphenicol. Cultures were grown 4 h or until an optical density at 600 nm (OD_{600}) of ~1 was achieved. The PAS812 OD_{600} was adjusted to match the library culture then diluted 1:1,000 into the library culture. The resulting mix was back-diluted 1:1,000 into 50 ml of LBPS-chloramphenicol and immediately split into two 25-ml volumes. Spectinomycin (50 μg/ml) was added to one culture, and both were grown overnight before centrifugation to collect bacterial pellets, which were stored at −80°C.

Library sequencing and odds ratio calculation. Genomic DNA was extracted from frozen cell pellets using a Qiagen DNeasy Blood & Tissue kit. Using genomic DNA as a template, trigger regions from HTMS libraries were amplified by PCR and sheared with a Covaris M220 ultrasonicator to 200- to 600-bp fragments. Sheared products were prepared using a New England Biolabs NEBNext Ultra II Prep kit and sequenced by Illumina MiSeq.

Raw reads were trimmed using Trimmomatic 0.36 (34) and aligned to a reference file (Data Sets S4 and S5 for MG1655 and Nissle 1917 libraries, respectively) using BWA mem 0.7.8 (35). The number of uniquely mapped reads for each trigger was counted.

The odds ratio is expressed as ($T_{x\text{-spect}}$/PNS_{spect})/(T_x/PNS), where T_x and $T_{x\text{-spect}}$ are the numbers of mapped reads for a particular trigger in the untreated and spectinomycin-treated cultures, respectively, and PNS and PNS_{spect} are the numbers of mapped reads for the positive normalization strain (PAS812) in the untreated and spectinomycin-treated cultures, respectively. Triggers with <5 reads in the gavage

suspension were discarded, unless they registered >20 reads at any subsequent time point. For each pair of untreated and spectinomycin-treated cultures (from a single fecal sample), odds ratios were calculated for each trigger with ≥5 reads in the untreated culture. The statistical significance was assessed with a one-tailed Fisher exact test (H_o, odds ratio = 0.02; H_a, odds ratio > 0.02). The odds ratio calculation compares each trigger only with itself (between spectinomycin-treated and untreated cultures), normalizing any sequencing length bias between triggers. It also normalizes to the positive normalization strain (PAS812) in each sample, negating read depth disparities between samples.

Data availability. Raw sequence data from library screening experiments have been deposited at the NCBI Sequence Read Archive as BioProject ID PRJNA542391. Other data and resources are available from the corresponding authors upon request.

SUPPLEMENTAL MATERIAL

Supplemental material for this article may be found at https://doi.org/10.1128/mSystems.00125-19.

FIG S1, EPS file, 0.3 MB.
FIG S2, EPS file, 0.2 MB.
FIG S3, EPS file, 0.3 MB.
FIG S4, EPS file, 0.3 MB.
DATA SET S1, XLSX file, 0.1 MB.
DATA SET S2, XLSX file, 0.1 MB.
DATA SET S3, XLSX file, 0.1 MB.
DATA SET S4, TXT file, 0.8 MB.
DATA SET S5, TXT file, 0.02 MB.

ACKNOWLEDGMENTS

REFERENCES

1. Ozdemir T, Fedorec AJH, Danino T, Barnes CP. 2018. Synthetic biology and engineered live biotherapeutics: toward increasing system complexity. Cell Syst 7:5–16. https://doi.org/10.1016/j.cels.2018.06.008.
2. Riglar DT, Silver PA. 2018. Engineering bacteria for diagnostic and therapeutic applications. Nat Rev Microbiol 16:214. https://doi.org/10.1038/nrmicro.2017.172.
3. Riglar DT, Giessen TW, Baym M, Kerns SJ, Niederhuber MJ, Bronson RT, Kotula JW, Gerber GK, Way JC, Silver PA. 2017. Engineered bacteria can function in the mammalian gut long-term as live diagnostics of inflammation. Nat Biotechnol 35:653–658. https://doi.org/10.1038/nbt.3879.
4. Daeffler KN, Galley JD, Sheth RU, Ortiz-Velez LC, Bibb CO, Shroyer NF, Britton RA, Tabor JJ. 2017. Engineering bacterial thiosulfate and tetrathionate sensors for detecting gut inflammation. Mol Syst Biol 13:923. https://doi.org/10.15252/msb.20167416.
5. Mimee M, Nadeau P, Hayward A, Carim S, Flanagan S, Jerger L, Collins J, McDonnell S, Swartwout R, Citorik RJ, Bulović V, Langer R, Traverso G, Chandrakasan AP, Lu TK. 2018. An ingestible bacterial-electronic system to monitor gastrointestinal health. Science 360:915–918. https://doi.org/10.1126/science.aas9315.
6. Hwang IY, Koh E, Wong A, March JC, Bentley WE, Lee YS, Chang MW. 2017. Engineered probiotic *Escherichia coli* can eliminate and prevent *Pseudomonas aeruginosa* gut infection in animal models. Nat Commun 8:15028. https://doi.org/10.1038/ncomms15028.
7. Mao N, Cubillos-Ruiz A, Cameron DE, Collins JJ. 2018. Probiotic strains detect and suppress cholera in mice. Sci Transl Med 10:eaao2586. https://doi.org/10.1126/scitranslmed.aao2586.
8. Mahan MJ, Slauch JM, Mekalanos JJ. 1993. Selection of bacterial virulence genes that are specifically induced in host tissues. Science 259:686. https://doi.org/10.1126/science.8430319.
9. Camilli A, Mekalanos JJ. 1995. Use of recombinase gene fusions to identify *Vibrio cholerae* genes induced during infection. Mol Microbiol 18:671–683. https://doi.org/10.1111/j.1365-2958.1995.mmi_18040671.x.
10. Khan MA, Isaacson RE. 2002. Identification of *Escherichia coli* genes that are specifically expressed in a murine model of septicemic infection. Infect Immun 70:3404–3412. https://doi.org/10.1128/IAI.70.7.3404-3412.2002.
11. Rediers H, Rainey PB, Vanderleyden J, Mot RD. 2005. Unraveling the secret lives of bacteria: use of *in vivo* expression technology and differ-

ential fluorescence induction promoter traps as tools for exploring niche-specific gene expression. Microbiol Mol Biol Rev 69:217–261. https://doi.org/10.1128/MMBR.69.2.217-261.2005.

12. Kotula JW, Kerns SJ, Shaket LA, Siraj L, Collins JJ, Way JC, Silver PA. 2014. Programmable bacteria detect and record an environmental signal in the mammalian gut. Proc Natl Acad Sci U S A 111:4838–4843. https://doi.org/10.1073/pnas.1321321111.

13. Naydich AD, Nangle SN, Bues JJ, Trivedi D, Nissar N, Inniss MC, Niederhuber MJ, Way JC, Silver PA, Riglar DT. 2019. Synthetic gene circuits enable systems-level biosensor discovery at the host-microbe interface. bioRxiv https://doi.org/10.1101/557934.

14. Noman N, Inniss M, Iba H, Way JC. 2016. Pulse detecting genetic circuit: a new design approach. PLoS One 11:e0167162. https://doi.org/10.1371/journal.pone.0167162.

15. Gimble FS, Sauer RT. 1985. Mutations in bacteriophage lambda repressor that prevent RecA-mediated cleavage. J Bacteriol 162:147.

16. Ziesack M, Karrenbelt MAP, Bues J, Schaefer E, Silver P, Way J. 2018. Escherichia coli NGF-1, a genetically tractable, efficiently colonizing murine gut isolate. Microbiol Resour Announc 7:e01416-18. https://doi.org/10.1128/MRA.01416-18.

17. McKenzie GJ, Craig NL. 2006. Fast, easy, and efficient: site-specific insertion of transgenes into enterobacterial chromosomes using Tn7 without need for selection of the insertion event. BMC Microbiol 6:39. https://doi.org/10.1186/1471-2180-6-39.

18. Engler C, Kandzia R, Marillonnet S. 2008. A one-pot, one-step, precision cloning method with high-throughput capability. PLoS One 3:e3647. https://doi.org/10.1371/journal.pone.0003647.

19. Mutalik VK, Guimaraes JC, Cambray G, Lam C, Christoffersen MJ, Mai Q-A, Tran AB, Paull M, Keasling JD, Arkin AP, Endy D. 2013. Precise and reliable gene expression via standard transcription and translation initiation elements. Nat Methods 10:354–360. https://doi.org/10.1038/nmeth.2404.

20. Zaslaver A, Bren A, Ronen M, Itzkovitz S, Kikoin I, Shavit S, Liebermeister W, Surette MG, Alon U. 2006. A comprehensive library of fluorescent transcriptional reporters for Escherichia coli. Nat Methods 3:623–628. https://doi.org/10.1038/nmeth895.

21. Hughes ER, Winter MG, Duerkop BA, Spiga L, Furtado de Carvalho T, Zhu W, Gillis CC, Büttner L, Smoot MP, Behrendt CL, Cherry S, Santos RL, Hooper LV, Winter SE. 2017. Microbial respiration and formate oxidation as metabolic signatures of inflammation-associated dysbiosis. Cell Host Microbe 21:208–219. https://doi.org/10.1016/j.chom.2017.01.005.

22. Winter SE, Lopez CA, Bäumler AJ. 2013. The dynamics of gut-associated microbial communities during inflammation. EMBO Rep 14:319–327. https://doi.org/10.1038/embor.2013.27.

23. Xu M, Busby SJW, Browning DF. 2009. Activation and repression at the Escherichia coli ynfEFGHI operon promoter. J Bacteriol 191:3172–3176. https://doi.org/10.1128/JB.00040-09.

24. Di Luccio E, Elling RA, Wilson DK. 2006. Identification of a novel NADH-specific aldo-keto reductase using sequence and structural homologies. Biochem J 400:105–114. https://doi.org/10.1042/BJ20060660.

25. Jain R, Yan Y. 2011. Dehydratase mediated 1-propanol production in metabolically engineered Escherichia coli. Microb Cell Fact 10:97. https://doi.org/10.1186/1475-2859-10-97.

26. Vogel-Scheel J, Alpert C, Engst W, Loh G, Blaut M. 2010. Requirement of purine and pyrimidine synthesis for colonization of the mouse intestine by Escherichia coli. Appl Environ Microbiol 76:5181–5187. https://doi.org/10.1128/AEM.00242-10.

27. Winkler JD, Garcia C, Olson M, Callaway E, Kao KC. 2014. Evolved osmotolerant Escherichia coli mutants frequently exhibit defective N-acetylglucosamine catabolism and point mutations in cell shape-regulating protein MreB. Appl Environ Microbiol 80:3729–3740. https://doi.org/10.1128/AEM.00499-14.

28. Zhang S, Jiao T, Chen Y, Gao N, Zhang L, Jiang M. 2014. Methylglyoxal induces systemic symptoms of irritable bowel syndrome. PLoS One 9:e105307. https://doi.org/10.1371/journal.pone.0105307.

29. Jones SA, Gibson T, Maltby RC, Chowdhury FZ, Stewart V, Cohen PS, Conway T. 2011. Anaerobic respiration of Escherichia coli in the mouse intestine. Infect Immun 79:4218–4226. https://doi.org/10.1128/IAI.05395-11.

30. Guymer D, Maillard J, Sargent F. 2009. A genetic analysis of in vivo selenate reduction by Salmonella enterica serovar Typhimurium LT2 and Escherichia coli K12. Arch Microbiol 191:519–528. https://doi.org/10.1007/s00203-009-0478-7.

31. Winter SE, Winter MG, Xavier MN, Thiennimitr P, Poon V, Keestra AM, Laughlin RC, Gomez G, Wu J, Lawhon SD, Popova IE, Parikh SJ, Adams LG, Tsolis RM, Stewart VJ, Bäumler AJ. 2013. Host-derived nitrate boosts growth of Escherichia coli in the inflamed gut. Science 339:708–711. https://doi.org/10.1126/science.1232467.

32. Datsenko KA, Wanner BL. 2000. One-step inactivation of chromosomal genes in Escherichia coli K-12 using PCR products. Proc Natl Acad Sci U S A 97:6640–6645. https://doi.org/10.1073/pnas.120163297.

33. Johnson JE, Lackner LL, Hale CA, de Boer P. 2004. ZipA is required for targeting of DMinC/DicB, but not DMinC/MinD, complexes to septal ring assemblies in Escherichia coli. J Bacteriol 186:2418–2429. https://doi.org/10.1128/jb.186.8.2418-2429.2004.

34. Bolger AM, Lohse M, Usadel B. 2014. Trimmomatic: a flexible trimmer for Illumina sequence data. Bioinformatics 30:2114–2120. https://doi.org/10.1093/bioinformatics/btu170.

35. Li H. 2013. Aligning sequence reads, clone sequences and assembly contigs with BWA-MEM. arXiv:13033997v2 [q-bio.GN] https://arxiv.org/abs/1303.3997.